Handling white-matter anisotropy in BEM for the EEG forward problem

Emmanuel Olivi, Théodore Papadopoulo, Maureen Clerc

HANDLING WHITE-MATTER ANISOTROPY IN BEM FOR THE EEG FORWARD PROBLEM

Emmanuel Olivi *Théodore Papadopoulo* *Maureen Clerc*

Athena Project Team, INRIA Sophia Antipolis Méditerranée, France

ABSTRACT

Solving the inverse problem of source localization in MEG or EEG, requires appropriate electrophysiological modeling of the head. Conductivity of tissues in the vicinity of the sources is especially influential on the MEG and EEG forward fields. Those tissues include white matter, whose conductivity is anisotropic because of its fiber structure. While white matter anisotropy can be measured thanks to Diffusion-Weighted MRI, it is rarely incorporated in MEG and EEG head models. Boundary Element Methods can only deal with piecewise constant conductivities, therefore ruling out white matter anisotropy that has a complex structure, and Finite Element Method have been developed to deal with anisotropic conductivity, but require very fine meshes, thus huge linear systems. The purpose of this paper is to extend the BEM framework to incorporate white matter anisotropy by treating anisotropic conductivity as a perturbation of an isotropic one.

***Index Terms*—** MEG, EEG, Boundary Element Method, Anisotropy, white matter

1. INTRODUCTION

MEEG (Magneto-ElectroEncephaloGraphy) is widely used for localizing non-invasively electrical sources within the brain. EEG measures the electric potential at electrodes placed on the scalp, whereas MEG measures the magnetic field in a radial direction with respect to the helmet. Solving an inverse problem of localization, *i.e.* finding the distribution of sources responsible for a given set of MEG or EEG measurements, requires a deep understanding of the electric conduction within the head. This volume conduction is represented by the forward problem which, for a known current distribution, provides the corresponding MEG or EEG measurements.

For the frequencies and the tissues of interest, the EEG forward problem amounts to a simple relation between the primary current source $\mathbf{J}_p$ and the electric potential V:

$$\nabla \cdot (\Sigma \nabla V) = \nabla \cdot \mathbf{J}_p. \tag{1}$$

The term $\Sigma\nabla V$ represents the Ohmic, extracellular, current flowing in a tissue with conductivity Σ. The electric potential also satisfies a homogeneous Neumann condition on the boundary (the scalp): $\Sigma\nabla V \cdot \mathbf{n} = 0$, expressing the fact that current does not flow outside the head (neglecting the neck), where $\mathbf{n}$ denotes the normal to the scalp.

Three main numerical methods are able to solve the forward problem with realistic geometries: the Finite Difference Method (FDM), the Finite Element Method (FEM) and the Boundary Element Method (BEM). FEM are able to deal with inhomogeneous, and anisotropic media, provided that a volumic mesh matching the different structures of the head is available. The geometric information used by BEM is the boundaries between tissues, but BEM can only consider a constant conductivity within each tissue.

The advantage of the BEM over the FEM resides in the easy handling of sources, and in the economical description of geometry. This translates into a huge user cost advantage that makes BEM the most used method for MEEG forward modeling. For isotropic head models, the symmetric BEM (sBEM) has recently been shown to have a better precision than other BEM [1] and than a standard tetrahedral FEM. BEM are however insufficient to handle anisotropic tissues, such as the skull, or more importantly still (for the MEG at least), the white matter. Yet, conductivity of tissues in the vicinity of the sources is especially influential on the MEG and EEG forward fields [2, 3]. This paper is a contribution to the handling of white matter conductivity within a BEM framework.

The outline is as follows: in Section 2, we present the conductivity model for white matter anisotropy, going from a tensor (volumic) description to a fiber (lineic) description. In Section 3, we show how white matter anisotropy can be viewed as a correction term to an isotropic model, and we present the numerical implementation via a BEM. Section 4 presents numerical results on a numerical model of a white matter fiber.

2. FROM TENSOR TO FIBERS

Tuch etal [4] have noticed a relationship between the diffusion tensor estimated by Diffusion-Weighted MRI, and the conductivity tensor. This allows one to use an anisotropic

Authors acknowledge support from ViMAGINE ANR-08-BLAN-0250-02 and the Regional Council of Provence-Alpes Côte d'Azur.

conductivity tensor for FEM. This tensor Σ is a rank-2 tensor, that can be represented as a matrix of dimension 3 ($\mathcal{M}_3(\mathbb{R})$), with only 6 degrees of freedom (due to symmetry): for any point x in the computational domain Ω,

$$\Sigma(x) \in \mathcal{M}_3(\mathbb{R}).$$

In an isotropic medium, the tensor is equivalent to a scalar σ. Writing χ_f the characteristic function of the fiber, such that:

$$\chi_f(x) = \begin{cases} 1 & \text{if } x \in f \\ 0 & \text{if } x \in \Omega \setminus f \end{cases},$$

In a small volume element $\mathbf{dv}$ containing a fiber with conductivity σ_f and a local direction $\mathbf{n}$, one can consider

$$\forall x \in \mathbf{dv},\ \Sigma(x) = \sigma I + (\sigma_f - \sigma)\, \chi_f(x) \mathbf{n}\mathbf{n}^T,$$

the tensor being decomposed as an isotropic term σI plus a correction term due to the fiber's conductivity. Axon bundles have a very small radius ($5.\,10^{-5}m$ on average) [5], and a typical element size in FEM is above $10^{-3}m$; the conductivity tensor used in FEM is a global description of smaller phenomena. Here, we propose to consider a fiber as a wire and to discretize it into fractions of wire, to which a local direction and a local conductivity can be assigned. For the remainder of the paper, only one fiber will be considered to simplify notations. A fiber f of length L assumed to have a constant radius r_f is discretized longitudinally with step l as:

$$\Delta_l(\chi_f) = l\pi r_f^2 \sum_{k=0}^{k=\frac{L}{l}} \delta_{kl},$$

where δ_{kl} denotes a Dirac positioned at the center of its section, at curvilinear abscissa kl.
The anisotropic conductivity tensor can now be split into an homogeneous part σI and a remainder due to the fractions of the fiber:

$$\forall x \in \Omega,\ \ \Sigma(x) = \sigma I + l\pi r_f^2 (\sigma_f - \sigma) \sum_{k=0}^{k=\frac{L}{l}} \delta_{kl} \mathbf{n}_k \mathbf{n}_k^T,$$

writing $\epsilon_f = l\pi r_f^2(\sigma_f - \sigma)$:

$$\forall x \in \Omega,\ \ \Sigma(x) = \sigma I + \epsilon_f \sum_{k=0}^{k=\frac{L}{l}} \delta_{kl} \mathbf{n}_k \mathbf{n}_k^T. \tag{2}$$

3. HANDLING A LOCAL ANISOTROPY IN BEM

From expression (2) of the conductivity tensor, the Poisson equation (1) becomes:

$$\nabla \cdot \Sigma \nabla V \ = \ \sigma \Delta V + \nabla \cdot \sum_{k=0}^{k=\frac{L}{l}} \delta_{kl} \epsilon_f \mathbf{n}_k \mathbf{n}_k^T \nabla V = \nabla \cdot \mathbf{J}_p$$

hence

$$\sigma \Delta V \ = \ \nabla \cdot \left(\mathbf{J}_p - \sum_{k=0}^{k=\frac{L}{l}} \delta_{kl} \epsilon_f \mathbf{n}_k \partial_{\mathbf{n}_k} V \right). \tag{3}$$

The correction term due to fibers is homogeneous to a current density as $\mathbf{J}_p$, and will be seen until the end of the paper, as a linear combination of virtual dipoles with positions kl and moments $\mathbf{m}_k = -\epsilon_f \mathbf{n}_k \partial_{\mathbf{n}_k} V$.
To solve problem (3), we consider an iterative scheme:

$$\sigma \Delta V^{n+1} \ = \ \nabla \cdot \left(\mathbf{J}_p - \sum_{k=0}^{k=\frac{L}{l}} \delta_{kl} \epsilon_f \mathbf{n}_k \partial_{\mathbf{n}_k} V^n \right), \tag{4}$$

with the initial condition $V^0 = 0$.
At the iteration $n = 0$, the problem is solved without the fiber contribution. At iteration $n = 1$, the term $\partial_{\mathbf{n}_k} V^0$ is computed, and then equation (4) is solved with the fiber acting as (virtual) dipoles. In this paper, only iterations $n = 0$ and $n = 1$ will be considered.

The symmetric BEM (sBEM) is built upon an extended Green representation theorem described in [6]. It uses boundary integral operators to relate the potentials and currents of the different interfaces. The EEG forward problem resolution with the sBEM makes use of these relations and solves for X in the equation $\mathtt{HeadMat} \cdot X = \mathtt{SourceMat}(\mathbf{J}_p)$. X denotes the sBEM variables at interfaces (potential and current), HeadMat is the matrix built with integral operators relating the sBEM variables, and $\mathtt{SourceMat}(\mathbf{J}_p)$ the matrix that projects the sources $\mathbf{J}_p$ onto the surfaces. The potential at sensors is then extracted from X. The Green representation theorem also makes it possible to compute the potential at any point in the domain (except at the precise location of the dipole, where the potential is indefinite) from X and the contribution of sources living in the same domain:
for $x \in \Omega$, $V(x) = \mathtt{Surf2V}_x \cdot X + \mathtt{Source2V}_x$, with Surf2V the internal operator, and Source2V the contribution of the sources. We will make use of this feature, to evaluate by finite difference, the partial derivative of V in the local direction of the fiber at a point x:

$$\partial_{\mathbf{n}} V(x) \simeq D_{d,\mathbf{n}} V(x) = \frac{V(x + \frac{d}{2}\mathbf{n}) - V(x - \frac{d}{2}\mathbf{n})}{d}.$$

Eq. (3), written with the sBEM operator now reads:

$$\mathtt{HeadMat} \cdot X = \mathtt{Source2Mat} \left(\mathbf{J}_p - \sum_{k=0}^{k=\frac{L}{l}} \delta_{kl} \epsilon_f \mathbf{n}_k D_{d,\mathbf{n}_k} V \right).$$

4. NUMERICAL VALIDATION

No analytical solution exists for the MEEG forward problem with local anisotropy. In order to validate the proposed BEM method with fibers, we have used a tetrahedral FEM and modeled a fiber oriented along the z-axis.

Head model description: the head model used is a 3-layer spherical model, representing the brain, the skull, and the scalp, with respective radii: $\{0.87,\ 0.92,\ 1.0\}$, and conductivities: $\{1.,\ 0.03,\ 1.\}$. Although both BEM and FEM can deal with non-spherical geometries, we have chosen the spherical model to minimize the difference between geometrical approximations of these two methods. A fiber was modeled as a cylinder with radius $R = 0.04$[1], starting at the point $[0.2,\ 0,\ -0.5]$ and ending at $[0.2,\ 0,\ 0.5]$ (in Cartesian coordinates), meaning a cylinder oriented along the z-axis, with length $L = 1$. A longitudinal conductivity of 10 is assigned to the fiber. We run the computations, for 16 dipoles located on the z-axis with z-coordinates in the set:

$$\{0.1,\ 0.2,\ 0.3,\ 0.4,\ 0.68,\ 0.765,\ 0.8015,\ 0.8415\},$$

and oriented either toward the Cartesian directions $[0,\ 0,\ 1]$ or $[1,\ 0,\ 1]$. This allows to see the influence of a fiber depending on the dipole location/orientation.

FEM model: the FEM used has tetrahedral elements, and represents the potential with P1 functions, and the solver is a preconditioned conjugate gradient. We run the simulation with a high number of elements, in order to achieve a good reference solution (mesh with 590 747 vertices obtained with CGAL[7]). The fiber was not meshed separately, so we have assigned to each finite element a conductivity depending on its (estimated) volume belonging to the cylinder. The number of tetrahedral elements entirely within the cylinder was 18 936 — 75%: 9 276 — 50%: 10 278 — 25%: 14 652.

BEM model: sBEM uses surfacic meshes. We generated spherical meshes with 642 vertices per mesh. The fiber was modeled as a succession of N virtual dipoles (discretization of the fiber *see* Eq. (2)), with a constant spacing on the z-axis: $1/N$ with $N = 100$.

Fig. 1, displays the head model used for the experiments. Some of the dipoles are represented on the z-axis, with green arrows for orientation $[0,\ 0,\ 1]$, and red arrows for $[1,\ 0,\ 1]$. A zoom on the fiber shows its discretization as virtual dipoles.

Comparisons between BEM and FEM is delicate. Methods do not run with the same type of element. We first show a result of the BEM and FEM using the same head model but without any fiber. For this head model, an analytical solution is available [8], and we are able to compare each numerical solution g_n, with the analytical one g_a. Comparisons are done using two measures, the RDM (Relative Difference Measure), and the MAG (Magnification error) defined as:

$$\mathrm{RDM}(g_a, g_n) = \left\| \frac{g_n}{\|g_n\|} - \frac{g_a}{\|g_a\|} \right\|, \quad \mathrm{MAG}(g_a, g_n) = \frac{\|g_n\|}{\|g_a\|},$$

For the RDM, the closer to 0 the better, and for the MAG the closer to 1, the better.

[1] All units used are SI units.

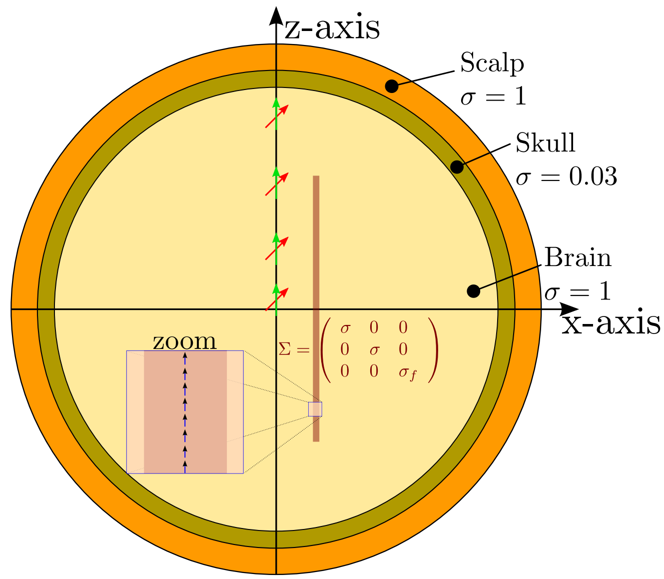

Fig. 1. Head model with a fiber

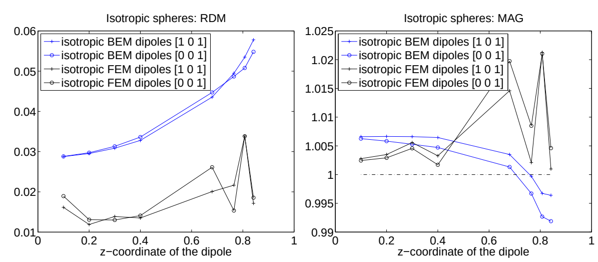

Fig. 2. Comparison of BEM and FEM with the analytical solution for an isotropic model. RDM (left), MAG (right).

One can see from Fig. 2 that FEM has a better RDM than BEM, whereas the MAG errors are comparable. The poor precision of the FEM regarding the MAG shows the difficulty of representing dipole amplitudes within FEM. In spite of its MAG, the FEM has better precision due to its very high number of elements, and will thus be used as a reference solution for the anisotropic case (with the fiber).

The black dashed line in Fig. 3 represents the error when comparing BEM to FEM in the isotropic case. We have just seen that FEM was more accurate than BEM when comparing to the analytical solution, thus taking the FEM as a reference solution leads to this black curve for a measure of accuracy of the isotropic BEM.

The blue line corresponds to the solution of the forward problem with BEM neglecting the fiber compared to the solution of FEM with the fiber. Finally the red line shows the BEM solution with the proposed method. For these dipoles oriented $[0,\ 0,\ 1]$, there is no big difference in the RDM between BEM with and without fiber, but the MAG, clearly shows an improvement when the fiber is modeled (the red

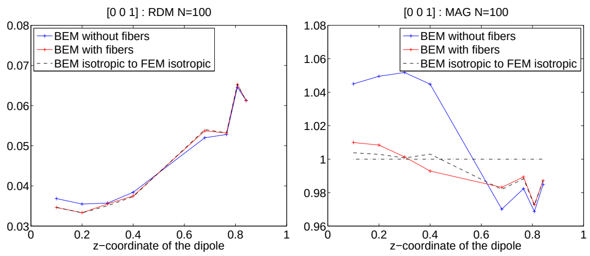

Fig. 3. Comparison of BEM to the FEM with the fiber for dipoles oriented $[0,\ 0,\ 1]$. RDM (left), MAG (right).

curve is closer to 1 than the blue one).

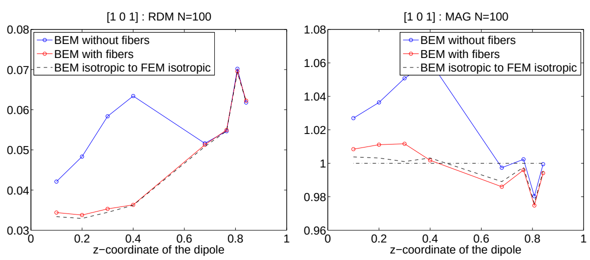

Fig. 4. Comparison of BEM to the FEM with the fiber for dipoles oriented $[1,\ 0,\ 1]$. RDM (left), MAG (right).

Fig. 4, for dipole orientation $[1,\ 0,\ 1]$, clearly demonstrates the influence of the virtual dipoles. Both RDM and MAG are significantly improved. Looking at the RDM, we see a gap between the BEM without fiber (in blue), and the BEM with fiber (in red), for the first dipoles. For dipoles with z-coordinates greater that 0.4, the three curves overlay, meaning that the fiber does not have much influence. The BEM solution with the fiber matches the previous comparison between BEM and FEM in the isotropic case (black dashed line). This means that the correction brought forth by the BEM fiber model is correct. We have also run the comparisons varying parameter of discretization N; and we have obtained similar results as long as $N > 20$.

5. CONCLUSION AND PERSPECTIVES

Studies have shown that anisotropic conductivity in the vicinity of the sources has a great influence both on EEG and on MEG forward solutions. In this paper, we have extended the BEM framework, allowing now for local anisotropy. The gain of the method was shown considering a single fiber that was not very close to the dipole, but the closer the fiber is, the greater its influence will be. Taking the anisotropic conductivity into account should improve significantly the forward/inverse problems in MEEG. Although in this paper, results have been shown only for EEG leadfields, the MEG leadfield may be handled similarly by making use of the Biot-Savart law. The white matter anisotropy representation presented here for the BEM makes an unprecedented bridge between MEEG and fiber tractography, through the linear discretization of the fibers. The proposed method may allow the MEEG community to take into account white matter anisotropy, without having to resort to very finely discretized FEM models.

6. REFERENCES

[1] A. Gramfort, T. Papadopoulo, E. Olivi, and M. Clerc, “OpenMEEG: opensource software for quasistatic bioelectromagnetics,” *BioMedical Engineering OnLine*, vol. 9, no. 45, Sept. 2010.

[2] C. H. Wolters, A. Anwander, X. Tricoche, D. Weinstein, M. A. Koch, and R. MacLeod, “Influence of tissue conductivity anisotropy on EEG/MEG field and return current computation in a realistic head model: A simulation and visualization study using high-resolution finite element modeling,” *NeuroImage*, vol. 30, no. 3, pp. 813–826, 2006.

[3] D Gullmar, J. Haueisen, F. Eiselt, M.and Giessler, L. Flemming, A. Anwander, T. Knosche, C. Wolters, Dumpelmann M., Tuch D., and Reichenbach J., “Influence of anisotropic conductivity on EEG source reconstruction: investigations in a rabbit model,” *IEEE Transactions on BioMedical Engineering*, vol. 53, no. 9, pp. 1841–1850, 2006.

[4] D.S Tuch, V.J. Wedeen, A.M. Dale, J.S. George, and J.W. Belliveau, “Conductivity tensor mapping of the human brain using diffusion tensor MRI,” in *Proceedings of the National Academy of Sciences*, 2001, vol. 98, pp. 11697–11701.

[5] K. Wang, S. Zhu, B. Mueller, K. Lim, Z. Liu, and B. He, “A new method to derive white matter conductivity from diffusion tensor mri.,” *IEEE Transactions BioMedical Engineering*, vol. 55, no. 10, pp. 2481–6, Oct. 2008.

[6] J. Kybic, M. Clerc, T. Abboud, O. Faugeras, R. Keriven, and T. Papadopoulo, “A common formalism for the integral formulations of the forward EEG problem,” *IEEE Transactions on Medical Imaging*, vol. 24, pp. 12–28, Jan. 2005.

[7] CGAL, “Computational geometry algorithms library,” http://www.cgal.org.

[8] Z. Zhang, “A fast method to compute surface potentials generated by dipoles within multilayer anisotropic spheres,” *Physics in Medicine and Biology*, vol. 40, pp. 335–349, 1995.